Structures of exotic ^{131,133}Sn isotopes and effect on r-process nucleosynthesis

Shi-Sheng Zhang,[1,2,3,*] M. S. Smith,[4,†] G. Arbanas,[5] and R. L. Kozub[6]

[1]*School of Physics and Nuclear Energy Engineering, Beihang University, Beijing 100191, China*
[2]*Institute of Theoretical Physics, Chinese Academy of Sciences, Beijing 100190, China*
[3]*Joint Institute for Heavy Ion Research, Oak Ridge National Laboratory, Oak Ridge, Tennessee 37831-6374*
[4]*Physics Division, Oak Ridge National Laboratory, Oak Ridge, Tennessee 37831-6354, USA*
[5]*Reactor and Nuclear Systems Division, Oak Ridge National Laboratory, Oak Ridge, Tennessee 37831-6171, USA*
[6]*Department of Physics, Tennessee Technological University, Cookeville, Tennessee 38505, USA*

Background: Four strong single-particle bound levels with strikingly similar level spacings have recently been measured in ^{131}Sn and ^{133}Sn. This similarity has not yet been addressed by a theoretical nuclear structure model. Information on these single-particle bound levels, as well as on resonant levels above the neutron capture threshold, is also needed to determine neutron capture cross sections—and corresponding capture reaction rates—on ^{130,132}Sn. The ^{130}Sn(n, γ) rate was shown in a recent sensitivity study to significantly impact the synthesis of heavy elements in the r-process in supernovae.

Purpose: Understand the structure of bound and resonant levels in ^{131,133}Sn, and determine if the densities of unbound resonant levels are sufficiently high to warrant statistical model treatments of neutron capture on ^{130,132}Sn.

Method: Single-particle bound and resonant levels for ^{131,133}Sn are self-consistently calculated by the analytical continuation of the coupling constant (ACCC) method based on a relativistic mean field (RMF) theory with BCS approximation.

Results: We obtain four strong single-particle bound levels in both ^{131,133}Sn with an ordering that agrees with experiments and spacings that, while differing from experiment, are consistent between the Sn isotopes. We also find at most one single-particle level in the effective energy range for neutron captures in the r-process.

Conclusions: Our RMF + ACCC + BCS model successfully reproduces observed single-particle bound levels in ^{131,133}Sn and self-consistently predicts single-particle resonant levels with densities too low for widely used traditional statistical model treatments of neutron capture cross sections on ^{130,132}Sn employing Fermi gas level density formulations.

Investigations of the evolution of shell structure in new regimes (e.g., new magic numbers, far from stability) are at the forefront of nuclear structure research. A recent study, for example, confirmed the doubly magic nature of ^{132}Sn through a measurement of four strong single-particle bound states populated via the (d, p) neutron transfer reaction on ^{132}Sn [1]. Using this same reaction on ^{130}Sn, four strong single-particle bound states were also recently observed in ^{131}Sn [2]. There is a striking similarity between the level spacings and strengths of these levels in ^{131,133}Sn (Fig. 1), a similarity not yet addressed by theory.

There is, furthermore, strong motivation to calculate levels *above* the neutron capture threshold in these Sn isotopes. Properties of single-particle *resonant* levels, not probed in these recent experiments [1,2] (or others [3]), are needed—along with bound levels—to determine neutron capture cross sections on ^{130,132}Sn. These are the basis for thermonuclear neutron capture reaction rates needed as input for simulations of r-process nucleosynthesis in supernovae [4]. The r-process is responsible for the production of half of the nuclides heavier than iron. In a recent study [5], variations of the

^{130}Sn(n, γ) capture rate were surprisingly shown to have a *global* impact on r-process simulations, changing final abundance calculations of nuclei over hundreds of mass units.

These capture cross sections have, however, large uncertainties. Global neutron capture cross sections have been calculated with statistical models (e.g., Refs. [6,7]), but it is uncertain whether there is a sufficiently high density of resonant levels [8] in ^{131,133}Sn for this approach to be valid for the r-process. Information on single-particle levels both above and below the ^{130,132}Sn neutron capture thresholds in ^{131,133}Sn are needed to understand and compare capture cross-section contributions from three mechanisms: direct neutron capture, capture through individual resonant states, and capture through closely spaced or overlapping resonances.

There are, however, no published calculations that uniformly and appropriately handle bound states *and* excited states above the neutron capture threshold for *both* ^{131}Sn and ^{133}Sn. The calculation of both sets of bound states is needed to understand the similarity of the level spacings as observed in recent experiments [1,2]; a treatment of bound levels and resonant levels is needed for improved neutron capture cross sections on ^{130,132}Sn that will impact calculations of heavy element abundances synthesized in the r-process.

There are several calculations of the structure of Sn isotopes in the vicinity of the $N = 82$ shell closure, with a variety

---
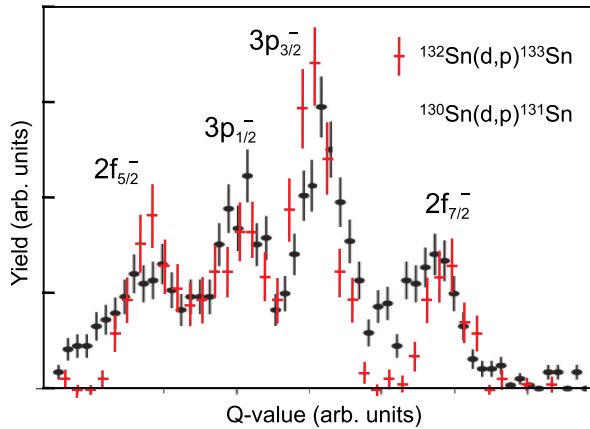
*zss76@buaa.edu.cn
†smithms@ornl.gov

FIG. 1. (Color online) Comparison of strong single-particle levels seen in recent ^{132}Sn$(d, p)^{133}$Sn [1] and ^{130}Sn$(d, p)^{131}$Sn [2] measurements.

of approaches including phenomenological, macroscopic-microscopic, microscopic, modified shell, and mean field models. Phenomenological approaches for levels in ^{133}Sn include the Koura-Yamada single-particle potential (KY-SPP) model [9] and a Nilsson potential model with new parameters [10]. Parameters in these models were adjusted to fit existing data of single-particle levels in the vicinities of doubly magic nuclides [9] or for $N = 3, 4,$ and 5 shells [10]. Since these two approaches give similar single-particle level calculations, we only show the Nilsson model [10] results in Fig. 2 for comparison below. Rauscher *et al.* [11] calculated bound levels in ^{133}Sn with the macroscopic finite-range droplet model (FRDM) with a folded-Yukawa (microscopic) potential and Lipkin-Nogami pairing. A microscopic Hartree-Fock-Bogoliubov (HFB) model [12] was also used in that work: nuclear states were determined by a variational procedure that simultaneously minimized the total energy with respect to single-particle wave functions and occupation factors. Jin *et al.* [13] made large-scale shell (LSS) model calculations on neutron-rich
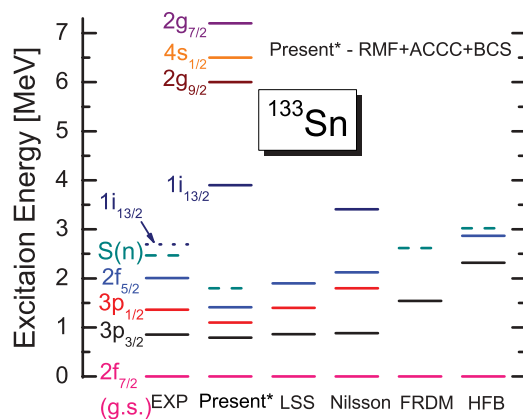

FIG. 2. (Color online) Bound levels and resonant levels in ^{133}Sn calculated by the RMF + ACCC + BCS approach with the NL3 effective interaction compared with the latest data [1,3] and calculations from the LSS [13], Nilsson [10], FRDM [11], and HFB [11] models. The available neutron capture thresholds $S(n)$ are also shown.

$A = 133$–135 nuclei. They used the NUSHELLX code [14] with a truncated model space ($2f_{7/2}$, $3p_{3/2}$, $1h_{9/2}$, $3p_{1/2}$, and $2f_{5/2}$ orbitals) and with core excitations determined by extended pairing-plus-quadrupole moments with monopole corrections. The model space truncation was necessary, because their calculations, which included ^{133}Sn, required too much memory if just one extra basis orbital—the $1i_{13/2}$—was included.

Another approach, relativistic mean field (RMF) theory, provides successful *global* descriptions of many properties of exotic nuclei [15], including binding energies, charge radii, and energies of bound levels. These models typically use ten interaction parameters that are fit to finite nuclear properties. Rauscher *et al.* [11] used the NLSH effective interaction [16] to calculate levels below the neutron capture threshold in ^{133}Sn. Zhang *et al.* [10] used the popular NL3 effective interaction [17] to determine levels above the $2f_{7/2}$ ground state and below the $1i_{13/2}$ excited state in ^{133}Sn; in ^{131}Sn, they only provide levels below the $2f_{7/2}$ state. The levels at $2f_{7/2}$ and above from these studies are shown for ^{133}Sn (^{131}Sn) in Fig. 2 (3) along with experimental data [1–3]. For ^{133}Sn, most previous investigations were primarily concerned with bound levels below the neutron capture threshold. Two studies [9,10] do consider the $1i_{13/2}$ orbital in ^{133}Sn, but no higher resonant states. In fact, the resonant states are the solution of a non-Hermitian Hamiltonian problem, corresponding to the second sheet of the complex energy plane with correct wave function asymptotic behavior. Methods for the *proper* solution of such problems are discussed in Ref. [18]. We note that *no* previous studies have considered resonant levels in ^{131}Sn, and that there is only tentative experimental evidence for the $1i_{13/2}$ level in ^{133}Sn [3], and no evidence for it in ^{131}Sn.

Positive energy single-particle states play a crucial role in the description of exotic nuclei because valence nucleons can be readily scattered into bound states above the Fermi surface and resonant states in the continuum. They are also required to determine the neutron capture cross sections needed for r-process simulations. It is advantageous to deduce the properties of unbound states from the eigenvalues and eigenfunctions of Hamiltonians for bound states, so that the methods developed for bound states can still be used and so that bound and resonant states are treated in a uniform way.

We follow this approach by employing the analytic continuation in the coupling constant (ACCC) [19] method to describe resonant states in ^{131,133}Sn. Here, a resonant state effectively becomes "bound" if the attractive potential is increased; this enables the energy, width, and wave function for the level to be determined by an analytic continuation carried out via a Padé approximant from the bound-state solutions [19]. The ACCC method can be easily implemented in conjunction with a variety of bound-state techniques. When coupled to the RMF model, this approach has been shown to work not only with narrow resonances, but also with broad resonances in which the phase shift $\delta(E)$ passes through $\pi/2$ smoothly and slowly [18]. The RMF + ACCC approach has been successfully used to describe the single-particle resonant states in ^{120}Sn [20]. An extension of this technique was recently developed to include pairing correlations by the Bardeen-Cooper-Schrieffer (BCS) approximation. This resonant-BCS model differs from the conventional BCS model in that only real resonant states $\sim 1\hbar\omega$

TABLE I. Comparison of single-particle level excitation energies E_x and energy spacings of adjacent levels ΔE_x from experimental measurements [1] and the present theoretical calculations of ^{133}Sn.

$J^{\pi a}$	E_x (keV)		ΔE_x (keV)	
	Expt.^{a}	Theory	Expt.^{a}	Theory
$7/2^-$	0	0		
$3/2^-$	854	792	854	792
$(1/2^-)$	1363 ± 31	1099	509 ± 31	307
$(5/2^-)$	2005	1415	642 ± 31	316

^{a}From Ref. [1].

TABLE II. Similar to Table I, but for ^{131}Sn, with experimental measurements from Ref. [2] and the present theoretical calculations (normalized to the $2f_{7/2}$ level).

$J^{\pi a}$	E_x (keV)		ΔE_x (keV)	
	Expt.^{b}	Theory^c	Expt.^{c}	Theory^c
$(7/2^-)$	2628	2628		
$(3/2^-)$	3404	3396	776	768
$(1/2^-)$	3986	3702	582	306
$(5/2^-)$	4655	4053	669	351

^{a}From Ref. [2].
$^b\pm 50$ keV [2].
^{c}Normalized to the experimental $2f_{7/2}$ level energy.

shell above the Fermi surface are included, and the spurious continuous states are kicked off from the continuum naturally [21,22]. Properties of bound levels and single-particle resonant states in Ni and Zr isotopes have been well described in a fully self-consistent way with this model [23,24].

Using our *global* RMF + ACCC + BCS approach, the single-particle bound and resonant levels in ^{131,133}Sn are calculated in a uniform manner with the NL3 effective interaction. Similar results are obtained with the NLSH effective interaction. Our results for ^{133}Sn are shown in Fig. 2 along with experimental data [1,3] and previous theoretical calculations; Table I gives our level energies and level spacings in comparison with measured values. Figure 3(a) and Table II give similar information for ^{131}Sn, and Fig. 3(b) compares our calculations for ^{131,133}Sn. We now discuss these results in detail.

The structure in ^{133}Sn was, according to the shell model, expected to have a series of strong single neutron levels outside a doubly magic ($Z = 50$, $N = 82$) core. Specifically, levels that are (nearly) pure $2f_{7/2}$, $3p_{3/2}$, $3p_{1/2}$, $1h_{9/2}$, and $2f_{5/2}$ orbitals were anticipated *if* the shell model holds for this unstable nucleus. This was verified in a measurement of ^{132}Sn$(d, p)^{133}$Sn [1], where four strong single-particle levels in ^{133}Sn were seen. On the basis of angular distributions, these levels were consistent with assignments to the $2f_{7/2}$, $3p_{3/2}$,

$3p_{1/2}$ and $2f_{5/2}$ orbitals [1]. Figure 2 shows these levels as well as the neutron capture threshold $S(n)$ at 2417 keV.

Our global RMF + ACCC + BCS model calculations with the NL3 effective interaction for ^{133}Sn agree with the levels and ordering below the neutron threshold. We estimate a lower value for the threshold (1800 keV), as well as lower energy spacings between the $3p_{3/2}$, $3p_{1/2}$, and $2f_{5/2}$ levels, than experimentally observed. As seen in Fig. 2, good agreement between theory and experiment is also obtained with the LSS model of Jin *et al.* [13] and the phenomenological Nilsson model. It is, however, expected that the agreement of the LSS model is good for $N = 3$ shell, because the inputs of the truncated model space (the $2f_{7/2}$, $3p_{3/2}$, $1h_{9/2}$, $3p_{1/2}$, and $2f_{5/2}$ orbitals) are taken from experimental data. The position of the $1i_{13/2}$ orbital in the Nilsson model is close to our calculation, but higher than the tentative experimental data. We note that the neutron capture threshold in the Nilsson model was not published.

As for ^{131}Sn, the expected level structure is more complicated than ^{133}Sn [3]. There is, for example, uncertainty about the spin-parity of the ground state, which is thought unlikely to have a pure single particle or hole configuration. The recent ^{130}Sn$(d, p)^{131}$Sn measurement did, however, show four strong single-particle levels (Fig. 1) [2]. On the basis of angular distributions, these levels were consistent with assignments to the $2f_{7/2}$, $3p_{3/2}$, $3p_{1/2}$, and $2f_{5/2}$ orbitals [2]—the same levels seen in ^{132}Sn$(d, p)^{133}$Sn [1]. Figure 3(a) shows these measured levels along with the 5247 keV neutron capture threshold energy $S(n)$. Due to the ground-state uncertainties, we have plotted energies relative to the $2f_{7/2}$ level. The relative level energies and spacings are given in Table II, and the similarity with levels in ^{133}Sn is shown in Fig. 3(b).

Our microscopic self-consistent RMF + ACCC + BCS calculations for ^{131}Sn, Fig. 3(a), agree with the experimental strong single-particle levels and their ordering below the neutron threshold. Consistent with our ^{133}Sn calculation, we obtain lower energy spacings between the $3p_{3/2}$, $3p_{1/2}$, and $2f_{5/2}$ levels in ^{131}Sn than experimentally observed [2], as well as an $S(n)$ value that is about 1 MeV lower than measured if normalized to $2f_{7/2}$.

Figure 3(b) shows a comparison of our predicted spacings of bound single-particle levels in ^{133}Sn and ^{131}Sn; numerical values are given in Tables I and II, respectively. Our model
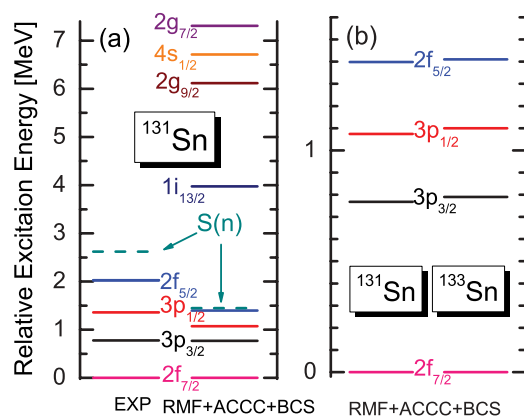

FIG. 3. (Color online) (a) Similar to Fig. 2, but for ^{131}Sn, with excitation energies relative to the $2f_{7/2}$ level. The results of the RMF + ACCC + BCS approach with the NL3 effective interaction are shown with the latest data [2]. (b) Comparison of present calculations for bound levels in ^{131,133}Sn.

successfully reproduces the similarity of the strong single-particle levels seen in the experimental spectra of these two nuclei (Fig. 1). Such similarities are not, however, the norm: the structures of ^{47,49}Ca across the $N = 28$ shell closure [3,25], for example, display significant changes in level spacings.

With our approach, we can estimate level energies both below and above the neutron capture threshold within the same formalism. Our calculations for the higher-lying $1i_{13/2}$, $2g_{9/2}$, $4s_{1/2}$, and $2g_{7/2}$ orbitals in ^{133}Sn are shown in Fig. 2. We predict the $1i_{13/2}$ to lie 2.2 MeV above the neutron capture threshold $S(n)$, whereas the tentative evidence for this level is at 0.2 MeV above $S(n)$. We predict the next lowest level to be the $2g_{9/2}$ level at 4.3 MeV above $S(n)$. As discussed above, no previous study considers all four higher-lying levels. The higher energy $1i_{13/2}$, $2g_{9/2}$, $4s_{1/2}$, and $2g_{7/2}$ orbitals from our calculations of ^{131}Sn are displayed in Fig. 3(a). We predict the two lowest energy resonances as the $1i_{13/2}$ ($2g_{9/2}$) levels, at energies 2.5 (4.7) MeV above $S(n)$, respectively.

There are numerous *qualitative* statements in the literature that for certain classes of nuclei—e.g., low mass, near shell closures, with low separation energies, or near the drip line—the density of levels will be too low for the assumption of closely spaced or overlapping resonances and averaged transmission coefficients to be valid. For such nuclei, the statistical model is inappropriate for cross-section calculations. A quantitative study [6,8] found that five s-wave levels—or ten levels of higher angular momentum transfer—per MeV were needed in the relevant excitation energy window to give a reasonable (20%) agreement between an integration over a level density and an exact sum over individual levels. The canonical excitation energy window of interest [26] for s-wave neutron captures on ^{130,132}Sn in the r-process is approximately 0.03–0.23 MeV above the neutron capture threshold in ^{131,133}Sn. This corresponds to the "effective energy" for capture at temperatures below 1.5 GK at which the r-process (n, γ) - (γ, n) equilibrium likely disappears and individual neutron capture cross sections influence the final abundance pattern [27]. For temperatures as high as 10 GK, this energy range will still only reach 1.5 MeV above threshold for s-wave capture. To reach 2.5 MeV above threshold, an "extended" window with temperatures of 2.0 GK and $l = 6$ captures are needed.

Our calculations give *no* single-particle levels within the canonical effective energy window for ^{131,133}Sn, and only one level—the $1i_{13/2}$, an $l = 6$ capture—within the extended window discussed above. This sparse level spacing suggests that approaches other than "traditional" statistical models—employing Fermi gas level density formulations—are needed to calculate neutron capture cross sections on both ^{130,132}Sn. We note that our analysis does not account for collective levels from, for example, particle-hole couplings or vibrational states. Such states do not play a role in widely used (e.g., Ref. [6]) level density formulations derived from the Fermi gas model [28], but are considered in more recent alternative level density models [29]. We also do not consider the level degeneracy splitting between substates that will occur as a result of the (slight) deformation of ^{131,133}Sn, but this will not significantly impact our level density results.

In summary, our RMF + ACCC + BCS model successfully reproduces the recently measured similarity of four observed strong single-particle bound levels in ^{131,133}Sn. We also predict no single-particle levels at energies above and near the neutron threshold, and only one level up to 2.5 MeV above the $S(n)$, which is a density of resonant levels that is too low to enable statistical models with Fermi gas level densities to calculate neutron capture cross sections. Our analysis suggests that alternative methods of calculating the neutron captures on ^{130,132}Sn must be utilized for r-process nucleosynthesis studies. This result also suggests the necessity for experimental measurements of level structures of heavy neutron-rich nuclei that are in and near the r-process.

[1] K. L. Jones *et al.*, Nature **465**, 454 (2010); Phys. Rev. C **84**, 034601 (2011).

[2] R. L. Kozub *et al.* (unpublished).

[3] http://www.nndc.bnl.gov.

[4] S. Goriely, Nucl. Phys. A **718**, 287c (2003).

[5] R. Surman, J. Beun, G. C. McLaughlin, and W. R. Hix, Phys. Rev. C **79**, 045809 (2009).

[6] T. Rauscher and F. K. Thielemann, At. Data Nucl. Data Tables **75**, 1 (2000).

[7] S. Goriely, S. Hilaire, and A. J. Koning, Astron. Astrophys. **487**, 767 (2008).

[8] T. Rauscher, F. K. Thielemann, and K. L. Kratz, Phys. Rev. C **56**, 1613 (1997).

[9] S. Chiba, H. Koura, T. Hayakawa, T. Maruyama, T. Kawano, and T. Kajino, Phys. Rev. C **77**, 015809 (2008).

[10] J. Y. Zhang, Y. Sun, M. Guidry, L. L. Riedinger, and G. A. Lalazissis, Phys. Rev. C **58**, R2663 (1998).

[11] T. Rauscher, R. Bieber, H. Oberhummer, K. L. Kratz, J. Dobaczewski, P. Moller, and M. M. Sharma, Phys. Rev. C **57**, 2031 (1998).

[12] J. Dobaczewski, I. Hamamoto, W. Nazarewicz, and J. A. Sheikh, Phys. Rev. Lett. **72**, 981 (1994)

[13] H. Jin, M. Hasegawa, S. Tazaki, K. Kaneko, and Y. Sun, Phys. Rev. C **84**, 044324 (2011).

[14] W. Rae, http://www.garsington.eclipse.co.uk/.

[15] J. Meng and P. Ring, Phys. Rev. Lett. **77**, 3963 (1996); J. Meng, Nucl. Phys. A **635**, 31 (1998).

[16] M. M. Sharma *et al.*, Phys. Lett. B **312**, 377 (1993); **317**, 9 (1993).

[17] G. A. Lalazissis, J. Konig, and P. Ring, Phys. Rev. C **55**, 540 (1997).

[18] S. S. Zhang, J. Meng, S. G. Zhou, and G. C. Hillhouse, Phys. Rev. C **70**, 034308 (2004).

[19] V. I. Kukulin, V. M. Krasnopl'sky, J. Horácek, *Theory of Resonances: Principles and Applications* (Kluwer Academic, Dordrecht, 1989).

[20] S. S. Zhang, Mod. Phys. Lett. A **19**, 1537 (2004).

[21] N. Sandulescu, L. S. Geng, H. Toki, and G. C. Hillhouse, Phys. Rev. C **68**, 054323 (2003).

[22] L. G. Cao and Z. Y. Ma, Eur. Phys. J. A **22**, 189 (2004).

[23] S. S. Zhang, Int. J. Mod. Phys. E **18**, 1761 (2009).

[24] S. S. Zhang, X. D. Xu, and J. P. Peng, Eur. Phys. J. A **48**, 40 (2012).

[25] B. A. Brown and W. A. Richter, Phys. Rev. C **58**, 2099 (1998).

[26] T. Rauscher, Phys. Rev. C **81**, 045807 (2010).

[27] R. Surman and J. Engel, Phys. Rev. C **64**, 035801 (2001).

[28] H. Bethe, Rev. Mod. Phys. **9**, 69 (1937).

[29] A. J. Koning, S. Hilaire, and S. Goriely, Nucl. Phys. A **810**, 13 (2008).